**Geoscientific
Model Development
Discussions**

Sensitivity of the Community Multiscale Air Quality (CMAQ) Model v4.7 results for the eastern United States to MM5 and WRF meteorological drivers

K. W. Appel, S. J. Roselle, R. C. Gilliam, and J. E. Pleim

Atmospheric Modeling and Analysis Division, National Exposure Research Laboratory, Office of Research and Development, US Environmental Protection Agency, RTP, NC 27711, USA

Correspondence to: K. W. Appel (appel.wyat@epa.gov)

GMDD

2, 1081–1114, 2009

Sensitivity of the Community Multiscale Air Quality

K. W. Appel et al.

Title Page

Abstract | Introduction

Conclusions | References

Tables | Figures

|◄ | ►|

◄ | ►

Back | Close

Full Screen / Esc

Printer-friendly Version

Interactive Discussion

Full Screen / Esc

Printer-friendly Version

Interactive Discussion

Abstract

This paper presents a comparison of the operational performances of two Community Multiscale Air Quality (CMAQ) model v4.7 simulations that utilize input data from the 5th-generation Mesoscale Model (MM5) and the Weather Research and Forecasting (WRF) meteorological models. Two sets of CMAQ model simulations were performed for January and August 2006. One set utilized MM5 meteorology (MM5-CMAQ) and the other utilized WRF meteorology (WRF-CMAQ), while all other model inputs and options were kept the same. For January, predicted ozone (O_3) concentrations were higher in the Southeast and lower Mid-west regions in the WRF-CMAQ simulation, resulting in slightly higher bias and error as compared to the MM5-CMAQ simulations. The higher predicted O_3 concentrations are attributed to less dry deposition of O_3 in the WRF-CMAQ simulation due to differences in the calculation of the vegetation fraction between the MM5 and WRF models. The WRF-CMAQ results showed better performance for particulate sulfate (SO_4^{2-}), similar performance for nitrate (NO_3^-) and total nitrate (TNO_3), and slightly worse performance for total carbon (TC) and total fine particulate ($PM_{2.5}$) mass than the corresponding MM5-CMAQ results. For August, predictions of O_3 were notably higher in the WRF-CMAQ simulation, particularly in the southern United States, resulting in increased model bias. Concentrations of predicted particulate SO_4^{2-} were lower in the region surrounding the Ohio Valley and higher along the Gulf of Mexico in the WRF-CMAQ simulation, contributing to poorer model performance. The primary cause of the differences in predicted concentrations between the MM5-CMAQ and WRF-CMAQ simulations is due to differences in the calculation of the friction velocity (u_*) in MM5 and WRF models, which has a large effect on the dry deposition of NO, NO_2 and HNO_3. Differences in the calculation of the vegetation fraction and the predicted cloud cover, along with several other minor differences in the simulations also affect the predicted concentrations from CMAQ. The performance for SO_4^{2-}, NO_3^- and NH_4^+ wet deposition was similar for both simulations for January and August.

1   Introduction

Air quality models, such as the Community Multiscale Air Quality (CMAQ) modeling system (Byun and Schere, 2006) and the Comprehensive Air Quality Model with extensions (CAMx) (ENVIRON, 2008), require gridded, high resolution (both temporally and spatially) meteorological data in order to accurately predict the transformation, transport and fate of pollutants in the atmosphere. Gridded Eulerian meteorological models, such as the 5th Generation Mesoscale Model (MM5; Grell et al., 1994) and the Weather Research and Forecasting model (WRF; Skamarock et al., 2008), are used to provide the meteorological data required by air quality models.

For the past 15 years, MM5 has been used to provide meteorological data for air quality simulations. The modular design of MM5 allows users to choose among various physics options such as: land-surface models (LSM), planetary boundary layer (PBL), radiation, microphysics and cloud schemes in order to optimize the model for a specific application. However, releases of new versions of MM5 by the community have ceased since the WRF model has taken its place. The WRF model incorporates the same capabilities as the MM5 model, but includes various improvements in the underlying dynamics of the model (e.g. mass conservation) along with updated physics, including new versions of the LSM, PBL, radiation and cloud microphysics schemes.

Although the WRF model has been available for several years and is being used operationally by the National Centers for Environmental Prediction (NCEP) and many other research groups, the model has seen limited use for retrospective air quality modeling applications. Until recently, operational performance of retrospective WRF model simulations has lagged that of MM5 simulations, due mostly to a lack of a comparable analysis nudging scheme. Analysis nudging is widely used by the air quality community to improve the performance of the meteorological simulations used in retrospective air quality simulations. A recently released version of an objective analysis utility for WRF (Obsgrid; Deng et al., 2008) improves the operational performance of retrospective WRF model simulations, making the performance comparable to MM5

(Gilliam and Pleim, 2009).

While other studies have compared the performance of air quality model predictions using different meteorological models (e.g. Smyth et al., 2006; de Meij et al., 2009), no studies have specifically compared the performance of MM5 and WRF driven CMAQ
5 model simulations. This study examines the operational performance of two sets of January and August 2006 CMAQ simulations, with one set using meteorological data provided by MM5 (MM5-CMAQ) and the other using data provided by the WRF model (WRF-CMAQ). The performance results for each simulation are presented and reasons for large differences in performance are discussed.

10 **2 Methodology**

2.1 MM5 and WRF model simulations

MM5 and WRF model simulations were performed for the eastern United States for January and August 2006 (with a 10 day spin-up period in the previous month) that utilize a horizontal grid with 12-km by 12-km grid cells and 34 vertical layers extending
15 up to 100 hPa. Boundary conditions for both the MM5 and WRF simulations were provided directly by the 12-km North American Model (NAM) simulation for the same time period. The details provided here regarding the MM5 and WRF model simulations are based on Gilliam and Pleim (2009), which compares the performance of similarly configured MM5 and WRF simulations as used in this study.
20 The MM5 simulation utilized version 3.7.4 of the model, with the Asymmetric Convective Model 2 (ACM2; Pleim, 2007a, b) PBL model, Pleim-Xiu (PX; Xiu and Pleim, 2001; Pleim and Xiu, 1995) LSM, Dudhia shortwave radiation scheme (Dudhia, 1989), RRTM longwave radiation scheme (Mlawer et al., 1997), Kain-Fritsch 2 (KF2; Kain, 2004) subgrid convective scheme and the Reisner-2 (Reisner et al., 1998) explicit microphysics
25 scheme. The PX LSM included indirect soil moisture and temperature nudging (Pleim and Xiu, 2003; Gilliam and Pleim, 2009). The similarly configured WRF model simula-

tion utilized the Advanced Research WRF (ARW) core version 3.0 (Skamarock et al., 2008), with the ACM2 PBL model, PX LSM, Dudhia shortwave and RRTM longwave radiation schemes, KF2 sub-grid convective scheme and the Thompson (Thompson et al., 2004) microphysics scheme. A summary of the configuration options for the MM5
5 and WRF model simulations is shown in Table 1. These options were chosen in order to obtain consistent performance for the two simulations, and are those options typically used by the MM5 and WRF communities, especially for retrospective air quality simulations.

2.2 CMAQ model simulations

10 The CMAQ model simulations were performed using CMAQv4.7 for the eastern United States for January and August 2006 using a three day spin-up period in the previous month on the same grid as the meteorology models except that its horizontal dimensions were reduced by 5 grid cells on each of the 4 lateral boundaries to avoid spurious boundary artifacts in the meteorology simulations. CMAQ was configured using the
15 AERO5 aerosol module and the CB05 chemical mechanism with chlorine chemistry extensions (Yarwood et al., 2005) and the ACM2 PBL scheme. The vertical layers for the CMAQ simulations match those of the meteorological simulations and therefore no vertical collapsing of layers was required. Version 3.4.1 of the Meteorology-Chemistry Interface Processor (MCIP; Otte et al., 2005) was used to process the MM5 and WRF
20 meteorology for use with CMAQ. The simulations used a 2005 base year emissions inventory which was updated with year specific mobile emissions and Constant Emissions Monitoring (CEM) data for point emissions for 2006. The latest version of the CMAQ model includes the option to calculate biogenic and plume rise emissions inline during the simulation, an option that was used for this study.

2.3 Model assessment techniques

The evaluation of the MM5, WRF and CMAQ model simulations was done primarily using the Atmospheric Model Evaluation Tool (AMET) (Appel and Gilliam, 2008). Meteorological predictions of 2-m temperature, 2-m water vapor mixing ratio and 10-m wind speed are paired in space and time with observations from the Meteorological Assimilation Data Ingest System (MADIS; http://madis.noaa.gov) database. The performance of the predictions is then assessed using available analyses in the AMET. Additionally, predicted monthly precipitation is compared against observations from the National Precipitation Analysis (NPA), which is a blend of radar estimated precipitation and rain gauge data (Fulton, 1998; Seo 1998a, b).

The CMAQ model predictions are paired in space and time with observations from the Environmental Protections Agency's (EPA) Air Quality System (AQS) for O_3, the Interagency Monitoring of PROtected Visual Environments (IMPROVE) network, the Chemical Speciation Network (CSN; previously called the Speciation Trends Network(STN)) and the Clean Air Status and Trends Network (CASTNet) for fine particulate matter, and the National Atmospheric Deposition Program (NADP) network for wet deposition species. Observations from the AQS (353 sites in January; 861 sites in August) are hourly; observations from the IMPROVE network (90 sites) and the CSN (174 sites in January; 157 sites in August) are daily average concentrations available every third day; CASTNet (67 sites) observations are weekly average concentrations, while the NADP network (202 sites) observations are weekly accumulated values.

Several statistical quantities are provided that assess the model bias and error. Root Mean Square Error (RMSE), Normalized Mean Error (NME), Normalized Median Error (NMdnE), Mean Error (ME) and Median Error (MdnE) are used to assess model error. Normalized Mean Bias (NMB), Normalized Median Bias (NMdnB), Mean Bias (MB) and Median Bias (MdnB) are used to assess model bias. The MdnB, MdnE, NMdnB and NMdnE are defined below as:

$$MdnB = \text{median} \left(C_M - C_O \right)_N \tag{1}$$

Printer-friendly Version

Interactive Discussion

$$MdnE = median \, |C_M - C_O|_N \tag{2}$$

$$NMdnB = \frac{median \, (C_M - C_O)_N}{median \, (C_O)_N} \times 100\% \tag{3}$$

$$NMdnE = \frac{median \, |C_M - C_O|_N}{median \, (C_O)_N} \times 100\% \tag{4}$$

where C_M and C_O are modeled and observed concentrations, respectively, and N is
the total number of model/observation pairs. Median is preferred here over mean since
median gives a better representation of the central tendency of the data than the mean
when analyzing data with non-normal distributions, which the observed PM species
data often are. Additional details regarding these statistics and how the observations
from the various observing networks are paired with CMAQ predictions and are used
in the AMET can be found in Appel et al. (2007, 2008).

3 MM5 and WRF model performance assessment

Since the objective of this study is to examine the differences between the MM5-CMAQ
and WRF-CMAQ predictions, it is important to determine what, if any, significant dif-
ferences exist between the MM5 and WRF model simulations from an operational per-
formance perspective. This section provides limited comparison of the MM5 and WRF
model performance, since a more detailed assessment of the MM5 and WRF model
performance can be found in Gilliam and Pleim (2009).

3.1 January

Figure 1a presents a comparison of the daily RMSE for 2-m temperature (T), water
vapor mixing ratio (w) and 10-m wind speed (WS) for January for the MM5 and WRF

model simulations. The RMSE for all three variables is very similar for January, although there are some periods where the RMSE for 2-m T is notably higher for the MM5 simulation. Figure 1b presents a comparison of the diurnal (hourly) bias for the same three variables for January. The WRF model simulation has much lower bias for

5 2-m T during the nighttime hours than the MM5 simulation, while the daytime bias is similar for the two simulations. The w bias is slightly lower in the WRF model simulation throughout most of the day, while the bias in 10-m WS is generally lower in the MM5 simulation. These analyses suggest that the WRF model is generally performing as well as the MM5 for these key meteorological variables for January.

10 A comparison of the observed accumulated monthly precipitation versus MM5 and WRF predicted precipitation for January is provided in Fig. 2a–c. The spatial pattern and amount of predicted precipitation from the MM5 (Fig. 2b) and WRF (Fig. 2c) model simulations are similar over land, and are generally comparable to the observed precipitation (Fig. 2a). The largest difference in predicted precipitation between the two

15 simulations occurs over the Gulf of Mexico and off the east coast of the United States, where the WRF model predicts much greater precipitation than MM5. It is not possible to determine which model is more correct, since the radar-based precipitation dataset is not available beyond the coast. However, the impact from the differences in the offshore precipitation on CMAQ predictions should be relatively small.

20 **3.2 August**

Figure 1c shows a comparison of the daily RMSE for 2-m T, w and 10-m WS for August for the MM5 and WRF simulations. The RMSE values for all three variables track very close to each other for most of the month. The RMSE for w is higher in both simulations for the first third of the month as compared to the other two-thirds

25 due to the higher moisture of the air-mass at the beginning of the month, after which a dryer air-mass dominated most of the eastern United States. The diurnal bias in 2-m T (Fig. 1d) is higher during the nighttime hours and lower during the daytime hours for the WRF simulation, while the w bias is significantly reduced in the WRF

Sensitivity of the Community Multiscale Air Quality

K. W. Appel et al.

Full Screen / Esc

Printer-friendly Version

Interactive Discussion

model simulation during most of the day. Although the bias in 10-m WS is similar throughout the afternoon, the MM5 simulation has slightly less bias during the overnight and early morning hours. See Gilliam and Pleim (2009) for additional details regarding the causes for the differences in performance.

Comparison of the monthly precipitation for August (Fig. 2d–f) shows greater variability compared to January, which is expected due to the convective nature of summertime precipitation. The WRF model simulation (Fig. 2f) predicts greater precipitation over the southeast United States and offshore as compared to the MM5 simulation (Fig. 2e) and the observations (Fig. 2d), while the MM5 simulation has slightly higher predicted precipitation over the lower Midwest as compared to WRF model simulation. Both models overpredict precipitation in the lower Midwest and underpredict precipitation in the upper Midwest and western Great Lakes regions. Overall, the performance of the MM5 and WRF model simulations for January and August is similar, and generally compares well with the observations. This result is similar to the conclusions of Gilliam and Pleim (2009), in which they note similar performance for the MM5 and WRF model simulations for the two months.

4 CMAQ model performance assessment

4.1 January

4.1.1 Ozone (O_3)

For January, O_3 predictions are generally higher in the WRF-CMAQ simulation, particularly across the southern portion of the model domain, where increases in monthly average O_3 of 2 ppb or more are present (Fig. 3a). The result is larger bias and error in the WRF-CMAQ simulation versus the MM5-CMAQ simulation (Table 2). Both simulations overpredict hourly O_3 on average, indicated by the positive NMdnB and MdnB for both simulations; however the NMdnB and MdnB are 3.7% and 0.85 ppb higher for

the WRF-CMAQ simulation, respectively. For maximum 8-h average O_3, the NMdnB and MdnB are 3.7% and 1.19 ppb higher for the WRF-CMAQ simulation. The error is similar between the two simulations for both measures of O_3.

Comparison of the O_3 dry deposition from the two simulations revealed that the higher predicted O_3 concentrations over the southern portion of the domain in WRF-CMAQ simulation are due to less O_3 dry deposition in the WRF-CMAQ simulation, which results in higher ambient O_3 concentrations. There are significant differences in the way the vegetation fraction and leaf area index (LAI) are parameterized in the PX LSM between the MM5 and WRF implementations. Both models use satellite-derived vegetation coverage to scale these vegetation parameters in areas dominated by crops. However, the parameterizations differ such that vegetation fraction and LAI are set to minimum values in the winter in all areas in WRF but maintain higher values in the southern-most areas (Gulf coast and Florida) in MM5. The result is less O_3 dry deposition in the WRF-CMAQ simulation due to less stomatal uptake (a result of the less vegetation and LAI) as compared to the MM5-CMAQ simulation, which in turn results in higher ambient O_3 concentrations. The WRF parameterization is being re-assessed and may be revised to be more like the MM5 parameterization in the future.

4.1.2   Fine particulate sulfate (SO_4^{2-})

Figure 3b shows the difference in the predicted monthly average concentrations of particulate SO_4^{2-} for January between the two CMAQ simulations. Predictions of SO_4^{2-} are generally higher in the WRF-CMAQ simulation, with the exception of a small area off the coast of southern Florida. The largest differences occur over the northern portion of the domain, where areas of greater than $1\,\mu g/m^3$ difference in monthly average SO_4^{2-} exist. While both simulations underpredict SO_4^{2-} on average (Table 2), the underprediction is smaller in WRF-CMAQ simulation, with a NMdnB that is 4.6–10.0% lower and a MdnB that is 0.05–0.20 $\mu g/m^3$ lower than in the MM5-CMAQ simulation. The error is also smaller in the WRF-CMAQ simulation, with the NMdnE 1.1–5.0% lower and the

MdnE 0.03–0.10 μg/m^3 lower than the MM5-CMAQ simulation.

The higher predicted concentrations of particulate SO_4^{2-} in the WRF-CMAQ simulation appear to be related to a combination of greater predicted cloud fraction and less SO_4^{2-} wet deposition (Fig. 4b) than in the MM5-CMAQ simulation. A comparison
5 of the resolved clouds between the MM5 and WRF model simulations reveal a large area over the upper Midwest and central Canada where the predicted cloud fraction in WRF is notably greater than MM5. The result is more in-cloud aqueous SO_4^{2-} production in that region, which results in the higher predicted SO_4^{2-} concentrations shown in Fig. 3b. The higher SO_4^{2-} concentrations along the east coast of the United States
10 and in Louisiana are also related to differences in the predicted cloud fraction. In the Northeast and eastern Canada, less SO_4^{2-} wet deposition (Fig. 4b) in the WRF-CMAQ simulation results in higher particulate SO_4^{2-} concentrations in that region.

4.1.3 Fine particulate nitrate (NO_3^-) and total nitrate (TNO_3)

NO_3^- tends to constitute the largest component of fine particulate mass in the eastern
15 United States during the cold season. Figure 3c shows the difference in monthly average NO_3^- between the two CMAQ model simulations for January. The WRF-CMAQ simulation predicts higher NO_3^- concentrations on average; however the differences are generally small, with only a few localized areas where the differences reach 1 μg/m^3 or greater. Since NO_3^- is underpredicted in both simulations (Table 2), the higher pre-
20 dicted concentrations in the WRF-CMAQ simulation result in an improvement of both the bias and error. The NMdnB is more than 10 % lower at the CSN sites in the WRF-CMAQ simulation as compared to the MM5-CMAQ simulation, while the difference in NMdnB at IMPROVE network sites is less than a percent. However, the difference in the NMdnE is larger at the IMPROVE network sites (5.4%) than at the CSN sites
25 (1.7%).

For TNO_3 (Fig. 3d), the differences between the two simulations are considerably

larger and more widespread than for NO_3^- alone, indicating significant differences in the HNO_3 predictions. The difference in predicted HNO_3 concentrations between the two simulations is likely the result of differences in the dry deposition velocity, which is very high for HNO_3 and limited primarily by the aerodynamic resistance. Aerodynamic resistance is strongly dependent on the friction velocity (u_*) that is, on average, higher in MM5 than WRF because MM5 has a higher minimum value for wind speed that is used in the friction velocity calculation. The higher friction velocity in MM5, particularly at night when wind speed is often very light, leads to greater dry deposition of HNO_3 for the MM5 based simulation. The consequently higher HNO_3 concentration predictions in the WRF-CMAQ simulation result in an increase in TNO_3 bias compared to the MM5-CMAQ simulation, as TNO_3 was already overpredicted in both simulations. The NMdnB and MdnB for TNO_3 at CASTNet sites are 9.1% and 0.21 $\mu g/m^3$ higher, respectively, in the WRF-CMAQ simulation. The NMdbE and MdnE are also higher in the WRF-CMAQ simulation, but to a slightly lesser degree.

4.1.4 Total carbon (TC)

Figure 3e shows the monthly average difference in TC between the two simulations for January. Differences are generally small and isolated; however, there are several areas where larger differences occur, specifically in the Northeast, along the Gulf of Mexico coast and in southern Florida. Although the differences in TC predictions are not very widespread, they do result in a larger bias at the CSN sites for the WRF-CMAQ simulation, with the NMdnB and MdnB 7.0% and 0.15 $\mu g/m^3$ higher, respectively, than the MM5-CMAQ simulation (Table 2). The error is also higher at the CSN sites in the WRF-CMAQ simulation. At the IMPROVE network sites, the bias and error are very similar between the two simulations. The larger bias at the CSN sites in the WRF-CMAQ simulation is due mainly to higher predicted TC concentrations in the Northeast, Great Lakes and Mid-Atlantic regions. Some of these differences are not apparent from Fig. 3e, as the average difference in TC between the two simulations is 0.15 $\mu g/m^3$,

which falls within the gray shading on the figure.

4.1.5   Total fine particulate mass (PM$_{2.5}$)

Figure 3f shows the monthly average difference in total PM$_{2.5}$ mass for January, which is dominated by the differences in SO$_4^{2-}$, TNO$_3$ and TC predictions already noted. The

5 MM5-CMAQ simulation has a slight bias in predicted total PM$_{2.5}$ mass (Table 2). The predicted total PM$_{2.5}$ mass is higher in the WRF-CMAQ simulation, which results in an increase in the NMdnB and MdnB of 5.0–8.6% and 0.21–0.87 μg/m^3, respectively.

Regarding the calculation of total PM$_{2.5}$mass from the raw CMAQ model output, PM$_{2.5}$ concentrations are calculated as a weighted sum of 40 different chemical species

10 tracked within the CMAQv4.7 aerosol module (Eq. 5).

$$PM_{2.5} = SO4_{i,j,k} + NO_{3i,j,k} + NH_{4i,j,k} + Na_{i,j,k} + Cl_{i,j,k}$$
$$+EC_{i,j} + 1.2\ ORGPA_{i,j} + SOA_j + Unspec_{j,k} + Soil_k \tag{5}$$

The subscripts i, j, and k represent the Aitken, accumulation, and coarse modes of the particle size distribution, respectively; Na represents a sum of all sea-salt cations, including sodium, potassium, magnesium, and calcium; ORGPA represents the directly-

15 emitted organic carbon; the multiplicative factor of 1.2 approximates the oxidation of ORGPA that occurs during atmospheric transport, a process that is not represented in CMAQ v4.7; SOA represents the sum of 19 secondary organic species described by Carlton et al. (2009); Unspec$_j$ and Unspec$_k$ are the model species A25J and ACORS, respectively, which represent directly-emitted PM that is not chemically speciated in the

20 national emissions inventory. In Eq. (5), each species with a subscript i is multiplied by a factor, PM25AT, to remove the portion of the Aitken mode mass distribution that exceeds 2.5 μm in aerodynamic diameter. Likewise, all species with subscript j are multiplied by PM25AC and the species with subscript k are multiplied by PM25CO. These three scaling factors have values between 0 and 1, which are computed in each grid

25 cell during each hour of the model simulation following the description by Jiang (2006), and written to the aerosol diagnostic output file.

4.1.6 Wet deposition species

Figure 4 shows the difference in the monthly precipitation and SO_4^{2-}, NO_3^- and NH_4^+ wet deposition for January between the two CMAQ model simulations. The largest differences in precipitation (Fig. 4a) are generally limited to areas over the Atlantic Ocean and Gulf of Mexico, with smaller differences occurring over the eastern United States. Most of the significant differences in precipitation over land occur in the southern portion of the domain, where the WRF model generally predicts less precipitation than MM5. The bias and error for precipitation (Table 2) is similar for both simulations, with the WRF simulation having slightly lower bias and error than the MM5 simulation.

The SO_4^{2-}, NO_3^- and NH_4^+ wet deposition are all lower in the WRF-CMAQ simulation, particularly in the Northeast, where large differences in precipitation were not observed. The SO_4^{2-} wet deposition shows the largest and most widespread decrease, which results in an unbiased NMdnB and MdnB for the WRF-CMAQ simulation, versus a NMdnB of 6.8% and MdnB of 0.01 kg/ha for the MM5-CMAQ simulation (Table 2). The NO_3^- and NH_4^+ wet deposition show smaller differences in bias between the two simulations, as expected. The error is generally comparable for the two simulations, with the WRF-CMAQ simulation having slightly lower error for SO_4^{2-} and NO_3^- wet deposition.

4.2 August

4.2.1 Ozone (O$_3$)

The difference in monthly average O_3 for August for the two CMAQ model simulations is shown in Fig. 5a. The predicted O_3 concentrations in the WRF-CMAQ simulation are higher throughout a large portion of the domain, particularly in the southern and western portions of the domain, while there are only a few isolated areas where O_3 concentrations were lower in the WRF-CMAQ simulation. The largest differences in predicted O_3 concentrations occur along the Gulf of Mexico, where the difference in

Full Screen / Esc

Printer-friendly Version

Interactive Discussion

predicted monthly average O_3 is greater than 4 ppb over a widespread area, with some isolated areas of greater than 10 ppb higher O_3. Both simulations overpredict O_3 (Table 2), however the overprediction is much larger for the hourly O_3 than the maximum 8-hr average O_3 due to large overpredictions of O_3 during the nighttime hours. As
5 expected, the bias is larger in the WRF-CMAQ simulation, with the NMdnB 4.2–4.9% higher and the MdnB 1.5–2.0 ppb higher than the MM5-CMAQ simulation. The error is also slightly higher in the WRF-CMAQ simulation. Figure 6a shows the difference in the mean bias of hourly O_3 (as compared to observations) at the AQS sites between the two simulations. The increase in mean bias is mainly limited to sites along the Gulf
10 Coast, where the mean bias at some sites increases by as much as 16 ppb. For the rest of the domain, the change in mean bias is generally small. However, some slightly larger increases in mean bias are noted in the upper Great Lakes region.

The higher predicted O_3 concentrations in the WRF-CMAQ simulation appear to be due to several differences between the MM5 and WRF model predictions. First, an
15 analysis of the predicted cloud fraction (CFRAC) from each simulation showed that the predicted CFRAC from the WRF-CMAQ simulation was on average less than that of the MM5-CMAQ simulation. The smaller CFRAC in the WRF-CMAQ simulation is favorable for greater O_3 production, as CFRAC is used in the calculation of the photolysis rate for O_3, and less CFRAC can result in increased O_3 photolysis. Although the CFRAC in
20 the WRF-CMAQ simulation was on average less than the MM5-CMAQ simulation, it is difficult to quantify the exact impact the difference in CFRAC played in the differences in O_3 concentrations between the two simulations.

Second, a comparison of surface solar radiation (SR) at the CASTNet sites showed that while both simulations overpredicted SR, the hourly SR during the daytime
25 (7 a.m. to 7 p.m.) was on average 20 watts/m^2 higher in the WRF-CMAQ simulation than in the MM5-CMAQ simulation for August, suggesting less overall cloud cover in the WRF-CMAQ simulation. The greater surface SR results in higher surface temperatures in the WRF-CMAQ simulation, which results in significantly greater concentrations of biogenic Volatile Organic Compounds (VOCs), which are highly sensitive to surface

temperature. The largest increase in VOCs in the WRF-CMAQ simulation (not shown) occurs along the Gulf of Mexico and through the upper Midwest, where the increase in the monthly average VOC concentrations is typically greater than 20%, with the concentrations in some areas more than doubling. The areas with large increases (>20%) in VOC concentrations in the WRF-CMAQ simulation correspond to those areas where O_3 concentrations were also much higher than in the MM5-CMAQ simulation.

A third difference between the MM5-CMAQ and WRF-CMAQ simulations that likely plays a role in the difference in the predicted O_3 concentrations (and other species as well) is the differences in the calculation of the u_* in each of the models, which was described previously in Sect. 4.1.3. The differences in the calculation of the u_* result in higher concentrations of NO and NO_2 (NO_x) in the WRF-CMAQ simulation, which is generally favorable for greater O_3 production. The combination of increased VOC and NO_x concentrations results in O_3 concentrations that are considerably higher across a large portion of the domain in the WRF-CMAQ simulation. The increase in O_3 may also be enhanced slightly along the Gulf of Mexico by a narrower and weaker sea-breeze front that was observed in the WRF model simulation, which results in less mixing along the coast. While other differences no doubt exist between the two simulations, these differences were identified as the most important factors contributing to the higher predicted O_3 concentrations in the WRF-CMAQ simulation.

4.2.2 Fine particulate sulfate (SO_4^{2-})

The difference in monthly average SO_4^{2-} between the two simulations for August is shown in Fig. 5b. There are two well-defined areas with significant differences in the predicted SO_4^{2-} concentrations; one being the area surrounding the Ohio Valley, where SO_4^{2-} concentrations are lower in the WRF-CMAQ simulation and the other being the area along the Gulf of Mexico, where SO_4^{2-} concentrations are higher in the WRF-CMAQ simulation. The result of the differences in SO_4^{2-} predictions is higher bias and error in the WRF-CMAQ simulation, with the NMdnB 1.5–8.2% higher and the MdnB

Full Screen / Esc

Printer-friendly Version

Interactive Discussion

0.02–0.39 μg/m^3 higher than the MM5-CMAQ simulation (Table 2). Figure 6b shows the spatial distribution of the difference in mean bias for SO$_4^{2-}$ at the IMPROVE network, CSN and CASTNet sites. As expected, the largest increase in bias for the WRF-CMAQ simulation occurs in the Ohio Valley and adjacent regions, while there is a small
5　improvement in the mean bias for sites along the Gulf of Mexico. The relatively dense collection of CASTNet sites in the Ohio Valley region results in the larger increase in bias and error for that network as compared to the CSN and IMPROVE networks (Table 2).

It was speculated that the lower predicted SO$_4^{2-}$ concentrations in the Ohio Valley
10　region in the WRF-CMAQ simulation were due to less aqueous-phase (in-cloud) production of SO$_4^{2-}$, while the increase in SO$_4^{2-}$ concentrations along the Gulf of Mexico were due to an increase in the gas-phase production of SO$_4^{2-}$. To test this hypothesis, the sulfur tracking version of CMAQ, which provides the concentration of SO$_4^{2-}$ from all the various sources (e.g. aqueous-phase, gas-phase, direct emissions, etc.) within the
15　CMAQ model was implemented for August. The results from the sulfur tracking version of CMAQ confirmed that the lower SO$_4^{2-}$ concentrations in the Ohio Valley region were due to less aqueous-phase SO$_4^{2-}$ production, while increase along the Gulf of Mexico was due to greater gas-phase SO$_4^{2-}$ production.

The reduced aqueous-phase production of SO$_4^{2-}$ concentrations in the WRF-CMAQ
20　simulation were due to the CMAQ sub-grid cloud model diagnosing fewer non-precipitating clouds than in the MM5-CMAQ simulation. A comparison of the precipitating and non-precipitating cloud fractions from CMAQ (available in the cloud diagnostic file) showed that the non-precipitating cloud fraction in the WRF-CMAQ model simulation was lower than that of the MM5-CMAQ simulation. Since non-precipitating clouds
25　can be a significant source of SO$_4^{2-}$ production in the atmosphere, it is likely that the lower SO$_4^{2-}$ concentrations in the WRF-CMAQ simulation are due to this decrease in non-precipitating clouds. The increase in SO$_4^{2-}$ along the Gulf of Mexico may be related to an increase in photolysis reactions in that area which results in higher OH concen-

Sensitivity of the Community Multiscale Air Quality

K. W. Appel et al.

Full Screen / Esc

Printer-friendly Version

Interactive Discussion

trations and an increase in the gas-phase production of SO_4^{2-} (which is also indicated by the higher O_3 concentrations in that region).

4.2.3 Fine particulate nitrate (NO_3^-) and total nitrate (TNO_3)

Figure 5c and d show the difference in monthly average NO_3^- and TNO_3 for August for the two CMAQ model simulations. NO_3^- and TNO_3 are both higher in the WRF-CMAQ simulation, with the largest increases occurring in the region surrounding the Great Lakes and along the Gulf of Mexico. The higher predicted NO_3^- and TNO_3 concentrations in the WRF-CMAQ simulation are likely due to less dry deposition of HNO_3 on average in the WRF-CMAQ simulation (a result of the difference in the calculation of u_* between the two models). The higher concentrations of predicted NO_3^- and TNO_3 in the WRF-CMAQ simulation result in a decrease in the bias in NO_3^-, which is largely underpredicted in both simulations, while the bias and error in TNO_3 predictions increase substantially compared to the MM5-CMAQ simulation (Table 3).

4.2.4 Total carbon (TC)

The largest differences in monthly average TC between the two simulations are generally limited to two regions, one along the Gulf of Mexico and the other in the upper Midwest (Fig. 5e). TC is largely underpredicted in both simulations (Table 3), and that underprediction is slightly less in the WRF-CMAQ simulation, with the NMdnB 5.2–6.7% lower and the MdnB 0.08–0.21 μg/m^3 lower than the MM5-CMAQ simulation. Differences in the predicted TC concentrations between the two simulations are likely related to the same factors that result in the higher O_3, SO_4^{2-} and TNO_3 concentrations.

4.2.5 Total fine particulate mass ($PM_{2.5}$)

Predictions of total $PM_{2.5}$ mass are on average higher in the WRF-CMAQ simulation for August (Table 3), which results in a small improvement in the bias and error, as $PM_{2.5}$

Printer-friendly Version

Interactive Discussion

mass is underpredicted in both simulations. The NMdnB and MdnB decrease by 2.2–7.0% and 0.27–0.83 μg/m^3, respectively, while the NMdnE and MdnE decrease by 2.0–4.2 % and 0.24–0.26 μg/m^3, respectively. The largest increase in PM$_{2.5}$ mass in the WRF-CMAQ simulation occurs along the Gulf of Mexico, where the increases in SO$_4^{2-}$,

5 TNO$_3$ and TC in that same region result in widespread monthly average differences in total PM$_{2.5}$ mass of more than 1 μg/m^3, and in some areas differences exceeding 5 μg/m^3 (Fig. 5f). There are some isolated areas in the Ohio Valley and surrounding regions where the PM$_{2.5}$ mass decreases by 1–2 μg/m^3 in the WRF-CMAQ simulation. Differences in PM$_{2.5}$ mass are due to the differences in the PM$_{2.5}$ constituent species

10 already discussed, along with differences in the prediction of the unspeciated mass.

4.2.6 Wet deposition species

The difference in monthly accumulated precipitation and SO$_4^{2-}$, NO$_3^-$ and NH$_4^+$ wet deposition for August is shown in Fig. 7. There are widespread differences in the predicted precipitation between the two simulations (Fig. 7a), much of which appears

15 to be due to differences in the prediction of the convective precipitation from the two models. The WRF model tends to forecast more precipitation over the southeastern portion of the domain, including over the Atlantic Ocean, Gulf of Mexico and Florida and along the Gulf Coast states, while the MM5 model predicts greater precipitation over the Midwest. Both models overpredict precipitation on average, with the WRF model

20 simulation having a smaller NMdnB and MdnB than the MM5 simulation (Table 3).

Differences in SO$_4^{2-}$ wet deposition are widespread and mixed throughout much of the domain (Fig. 7b). Greater SO$_4^{2-}$ wet deposition occurs over the Southeast and along the Gulf of Mexico in the WRF-CMAQ simulation, which correlates to regions where greater precipitation was observed as well, while there are areas in the Mid-

25 west with less SO$_4^{2-}$ wet deposition in the WRF-CMAQ simulation, which correlate to areas where less precipitation was also predicted. There are, however, also large differences in SO$_4^{2-}$ wet deposition in the Northeast, a region where large differences in

precipitation were not observed. It is not immediately apparent what the cause of these differences is, and requires further investigation. Overall, the performance for SO_4^{2-} wet deposition at the NADP network sites is slightly better for the WRF-CMAQ simulation, with slightly less bias and error as compared to the MM5-CMAQ simulation (Table 3). The NO_3^- and NH_4^+ wet deposition (Fig. 9c and d) show similar patterns to the SO_4^{2-} wet deposition, although with much smaller absolute differences. The performance for those species is also slightly better for the WRF-CMAQ simulation (Table 3).

5 Summary

Two sets of CMAQv4.7 simulations were performed for January and August 2006, with one set using the MM5 meteorology and the other set using WRF model meteorology. Predictions from the CMAQ model simulations were compared against observations from various networks and the performance for each set of simulations was assessed and compared against the other set. For January, performance differences in the predicted O_3 concentrations from each simulation were caused by differences in the calculation of the vegetation fraction between the two simulations, which results in differences in the amount of O_3 dry deposition taking place in each simulation. Higher predicted concentrations of SO_4^{2-} in January in the WRF-CMAQ simulation are likely related to a combination of more predicted cloud cover, which results in an increase in the amount of aqueous-phase (in-cloud) SO_4^{2-} produced, and less SO_4^{2-} wet deposition as compared to the MM5-CMAQ simulation. Predictions of NO_3^- and TNO_3 were also higher in the WRF-CMAQ simulation due to less dry deposition of HNO_3 in the WRF-CMAQ simulation, a result of differences in the calculation of the u_* in the MM5 and WRF models.

For August, the WRF-CMAQ simulation generally underperformed compared to the MM5-CMAQ simulation. The bias in O_3 was higher in the WRF-CMAQ simulation, with the largest increases in bias occurring in the southeast United States, particularly in Florida, along the Gulf of Mexico and in Texas. The increase in predicted O_3 concen-

◄ | ►►

◄ | ►

Back | Close

Full Screen / Esc

Printer-friendly Version

Interactive Discussion

trations in the WRF-CMAQ simulation appears to be most directly related to greater predicted surface SR (due to fewer predicted clouds) in the WRF-CMAQ simulation, which results in higher surface temperatures and an increase in the concentration of surface biogenic VOCs. Additionally, the smaller predicted CFRAC in the WRF-CMAQ
5 simulation results in an increase in the amount of O_3 photolysis taking place.

Predicted concentrations of SO_4^{2-}, which were already underpredicted in both simulations, were lower in the WRF-CMAQ simulation in the Ohio Valley region, but higher along the Gulf coast states. The decrease in predicted SO_4^{2-} concentrations in the WRF-CMAQ simulation is likely related to fewer predicted non-precipitating clouds in
10 the WRF-CMAQ simulation, which results in less aqueous-phase production of SO_4^{2-} in the Midwest and Ohio Valley, while the increase along the Gulf of Mexico is due to greater gas-phase production of SO_4^{2-}. Predicted concentrations of NO_3^- and TNO_3 were higher in the WRF-CMAQ simulation, primarily due to increased concentrations of NO_x and HNO_3 from less dry deposition of those species (due to differences in the
15 u_* calculation) and to a lesser extent an increase in nitrite replacement in response to lower predicted SO_4^{2-} concentrations.

The most significant differences in the meteorological predictions are related to the calculation of u_*, the amount of atmospheric moisture present and the predicted cloud cover, all of which contribute to differences in the CMAQ model predictions. Additional
20 exploration of these differences and how they impact the CMAQ model predictions is needed. This could be accomplished by extending the comparison to an annual simulation, which would capture differences in the spring and fall. Additionally, an analysis of the performance for the western United States would be beneficial.

Disclaimer – The United States Environmental Protection Agency through its Office of

Research and Development funded and managed the research described here. It has been subjected to Agency review and approved for publication.

References

Appel, K. W., Bhave, P. V., Gilliland, A. B., Sarwar, G., and Roselle, S. J.: Evaluation of the Community Multiscale Air Quality (CMAQ) model version 4.5: Sensitivities impacting model performance; Part II – particulate matter, Atmos. Environ., 42, 6057–6066, 2008.

Appel, K. W., Gilliland, A. B., Sarwar, G., and Gilliam, R. C.: Evaluation of the Community Multiscale Air Quality (CMAQ) model version 4.5: Sensitivities impacting model performance: Part I – Ozone, Atmos. Environ., 41, 9603–9615, 2007.

Appel, K. W. and Gilliam, R. C.: Overview of the Atmospheric Model Evaluation Tool (AMET). 7th Annual CMAS Conference, Chapel Hill, NC, 6–8 October 2008, http://www.cmascenter.org/conference/2008/agenda.cfm, 2008.

Byun, D. W. and Schere, K. L.: Review of the governing equations, computational algorithms, and other components of the Models-3 Community Multiscale Air Quality (CMAQ) modeling system, Appl. Mech. Rev., 55, 51–77, 2006.

Carlton, A. M. G., Bhave, P. V., Napelenok, S. L., Pinder, R. W., Sarwar, G., Pouliot, G. A., Edney, E. O., and Houyoux, M.: Improved Treatment of Secondary Organic Aerosols in CMAQ, Environ. Sci. Technol., submitted, 2009.

de Meij, A., Gzella, A., Thunis, P., Cuvelier, C., Bessagnet, B., Vinuesa, J. F., and Menut, L.: The impact of MM5 and WRF meteorology over complex terrain on CHIMERE model calculations, Atmos. Chem. Phys. Discuss., 9, 2319–2380, 2009, http://www.atmos-chem-phys-discuss.net/9/2319/2009/.

Deng, A., Stauffer, D.R., Dudhia, J., Hunter, G.K., and Bruyere, C.: WRF-ARW analysis nudging update and future development plan. 9th Annual WRF Users' Workshop, Boulder, CO, 23–27 June 2008, http://www.mmm.ucar.edu/wrf/users/workshops/WS2008/abstracts/1-06.pdf.

Dudhia, J.: Numerical study of convection observed during the winter monsoon experiment using a mesoscale two-dimensional model, J. Atmos. Sci., 46, 3077–3107, 1989.

ENVIRON: User's Guide to the Comprehensive Air Quality Model with Extensions (CAMx) Version 4.50. ENVIRON International Corporation, 773 San Marin Drive, Suite 2115 Novato, California 94998. Available at http://www.camx.com/files/CAMxUsersGuide_v4.50.pdf, 2008.

Fulton, R. A., Breidenbach, J. P., Seo, D. J., Miller, D. A., and O'Bannon, T.: The WSR-88D rainfall algorithm, Weather Forecasting, 13, 377–395, 1998.

Gilliam, R. C. and Pleim, J. E.: Performance assessment of new land-surface and planetary boundary layer physics in the WRF-ARW, J. Appl. Meteor. Clim., in review, 2009.

5 Grell, G. A., Dudhia, A. J., and Stauffer, D. R.: A description of the Fifth-Generation PennState/NCAR Mesoscale Model (MM5). NCAR Technical Note NCAR/TN-398+STR. Available at http://www.mmm.ucar.edu/mm5/doc1.html, 1994.

Jiang, W., Smyth, S., Giroux, E., Roth, H., and Yin, D.: Differences between CMAQ fine mode particle and $PM_{2.5}$ concentrations and their impact on model performance evaluation in the 10 lower Fraser valley, Atmos. Environ., 40, 4973–4985, 2006.

Kain, J. S.: The Kain-Fritsch convective parameterization: An update, J. Appl. Meteor., 43, 170–181, 2004.

Mlawer, E. J., Taubman, S. J., Brown, P. D., Iacono, M. J., and Clough, S. A.: Radiative transfer for inhomogeneous atmosphere: RRTM, a validated correlated-k model for the long-wave, J. 15 Geophys. Res., 102(D14), 16663–16682, 1997.

Otte, T. L., Pouliot, G., Pleim, J. E., Young, J. O., Schere, K. L., Wong, D. C., Lee, P. C. S., Tsidulko, M., McQueen, J. T., Davidson, P., Mathur, R., Chuang, H. Y., DiMego, G., and Seaman, N. L.: Linking the Eta model with the Community Multiscale Air Quality (CMAQ) modeling system to build a national air quality forecasting system, Weather Forecasting, 20, 20 367–384, 2005.

Pleim, J. E. and Xiu, A.: Development and testing of a surface flux and planetary boundary layer model for application in mesoscale models, J. Appl. Meteor., 34, 16–32, 1995.

Pleim, J. E. and Xiu, A.: Development of a Land-surface Model. Part II: Data Assimilation, J. Appl. Meteor., 42, 1811–1822, 2003.

25 Pleim, J. E.: A combined local and nonlocal closure model for the atmospheric boundary layer. Part I: model description and testing, J. Appl. Meteor. Clim., 46, 1383–1395, 2007a.

Pleim, J. E.: A combined local and nonlocal closure model for the atmospheric boundary layer, Part II: application and evaluation in a mesoscale meteorological model, J. Appl. Meteor. Clim., 46, 1396–1409, 2007b.

30 Reisner, J., Rasmussen, R. M., and Bruintjes, R. T.: Explicit forecasting of supercooled liquid water in winter storms using the MM5 mesoscale model, Q. J. Roy. Meteor. Soc., 124, 1071–1107, 1998.

Seo, D. J.: Real-time estimation of rainfall fields using rain gauge data under fractional coverage

conditions, J. Hydrol., 208, 25–36, 1998a.

Seo, D. J.: Real-time estimation of rainfall fields using radar rainfall and rain gauge data, J. Hydrol., 208, 37–52, 1998b.

Skamarock, W. C., Klemp, J. B., Dudhia, J., Gill, D. O., Barker, D. M., Duda, M. G., Huang, X.-Y., Wang, W., and Powers, J. G.: A description of the advanced research WRF version 3. NCAR Tech Note NCAR/TN 475 STR, 125 pp., [available from UCAR Communications, P.O. Box 3000, Boulder, CO 80307, USA], 2008.

Smyth, S. C., Yin, D., Roth, H., Jiang, W., Moran, M. D., and Crevier, L. P.: The impact of GEM and MM5 modeled meteorological conditions on CMAQ air quality modeling results in Eastern Canada and the Northeastern United States, J. Appl. Meteor. Clim., 45, 1525–1541, 2006.

Thompson, G., Rasmussen, R. M., and Manning, K.: Explicit forecasts of winter precipitation using an improved bulk microphysics scheme. Part I: Description and sensitivity analysis, Mon. Weather Rev., 132, 519–542, 2004.

Xiu, A. and Pleim, J. E.: Development of a land-surface model. Part I: application in a mesoscale meteorological model, J. Appl. Meteor., 40, 192–209, 2001.

Yarwood, G., Roa, S., Yocke, M., and Whitten, G.: Updates to the carbon bond chemical mechanism: CBo5. Final report to the US EPA, RT-0400675, available at http://www.camx.com, 2005.

Sensitivity of the Community Multiscale Air Quality

K. W. Appel et al.

Title Page

Abstract | Introduction

Conclusions | References

Tables | Figures

|◄ | ►|

◄ | ►

Back | Close

Full Screen / Esc

Printer-friendly Version

Interactive Discussion

K. W. Appel et al.

Table 1. Options used for the MM5 and WRF model simulations.

Model	MM5	WRF
Version	v3.7.4	ARW core v3.0
Grid Spacing	12 km×12 km	12 km×12 km
PBL Model	ACM2	ACM2
LSM	Pleim-Xiu	Pleim-Xiu
Sub-grid Convection Scheme	Kain-Fritsch 2	Kain-Fritsch 2
Shortwave Radiation Scheme	Dudhia	Dudhia
Longwave Radiation Scheme	RRTM	RRTM
Explicit Microphysics Scheme	Reisner 2	Thompson
Objective Analysis Approach	Rawins	OBSGRD

Table 2. Statistics of RMSE, NMdnB, NMdnE, MdnB and MdnE for fine particulate and wet deposition species for January 2006. MM5 indicates the MM5-CMAQ simulation; WRF indicates the WRF-CMAQ simulation. MdnB and MdnE values are in ppb for O_3, $\mu g/m^3$ for aerosol species, mm for precipitation and kg/ha for wet deposition species.

Species	Network	# of Obs	NMdnB (%) MM5	WRF	NMdnE (%) MM5	WRF	MdnB MM5	WRF	MdnE MM5	WRF
O_3 (Hourly)	AQS	245 129	8.2	11.9	25.4	26.5	1.88	2.73	5.85	6.10
O_3 (8-h Max)		9925	1.5	5.2	12.9	12.8	0.5	1.69	4.19	4.16
SO_4^{2-}	IMPROVE	691	−7.0	−2.4	21.9	19.2	−0.08	−0.03	0.25	0.22
	CSN	988	−13.1	−5.4	24.6	23.5	−0.29	−0.12	0.55	0.52
	CASTNet	247	−12.8	−2.8	17.3	12.3	−0.26	−0.06	0.35	0.25
NO_3^-	IMPROVE	691	−8.7	−7.8	73.0	67.6	−0.03	−0.03	0.27	0.25
	CSN	953	−17.1	−6.8	47.6	45.9	−0.25	−0.10	0.69	0.66
TNO_3	CASTNet	247	8.3	17.4	19.1	21.6	0.19	0.40	0.43	0.49
TC	IMPROVE	727	−17.1	−16.6	42.3	41.4	−0.14	−0.14	0.35	0.34
	CSN	905	7.2	14.2	37.9	43.0	0.14	0.29	0.77	0.87
$PM_{2.5}$	IMPROVE	750	5.7	10.7	35.6	38.6	0.23	0.44	1.45	1.57
	CSN	868	1.4	10	27.9	30.7	0.14	1.01	2.82	3.10
Precipitation		706	7.0	3.4	44.8	40.6	0.62	0.30	3.99	3.61
WetD Sulf.		572	6.8	0.0	49.2	44.6	0.01	0.00	0.06	0.06
WetD Amm.	NADP	572	−17.0	−16.1	49.5	49.6	0.00	0.00	0.01	0.01
WetD Nitr.		572	2.7	−2.6	47.1	45.1	0.00	0.00	0.06	0.06

Table 3. Statistics of RMSE, NMdnB, NMdnE, MdnB and MdnE for fine particulate and wet deposition species for August 2006. MM5 indicates the MM5-CMAQ simulation; WRF indicates the WRF-CMAQ simulation. MdnB and MdnE values are in ppb for O_3, $\mu g/m^3$ for aerosol species, mm for precipitation and kg/ha for wet deposition species.

Species	Network	# of Obs	NMdnB (%) MM5	NMdnB (%) WRF	NMdnE (%) MM5	NMdnE (%) WRF	MdnB MM5	MdnB WRF	MdnE MM5	MdnE WRF
O_3 (Hourly)	AQS	598 583	14.1	19.0	28.9	31.1	4.36	5.88	8.95	9.65
O_3 (8-h Max)		24413	1.2	5.4	13.3	14.2	0.57	2.62	6.47	6.89
SO_4^{2-}	IMPROVE	531	−8.5	−10.0	38.5	34.5	−0.12	−0.14	0.53	0.48
	CSN	932	−6.7	−7.5	25.0	24.1	−0.24	−0.25	0.89	0.86
	CASTNet	251	−11.8	−20.0	14.9	21.6	−0.57	−0.96	0.72	1.04
NO_3^-	IMPROVE	531	−51.7	−45.4	73.0	71.2	−0.07	−0.06	0.10	0.10
	CSN	892	−45.2	−31.4	63.0	59.6	−0.18	−0.12	0.25	0.24
TNO_3	CASTNet	251	10.9	29.3	32.0	42.0	0.18	0.48	0.52	0.68
TC	IMPROVE	701	−47.7	−42.5	53.5	47.6	−0.71	−0.63	0.80	0.71
	CSN	896	−44.7	−38.0	46.9	41.9	−1.40	−1.19	1.47	1.31
$PM_{2.5}$	IMPROVE	693	−32.7	−28.5	38.2	34.0	−2.10	−1.83	2.45	2.19
	CSN	809	−22.1	−15.1	30.9	28.9	−2.65	−1.82	3.71	3.47
Precipitation		705	18.3	6.8	94.6	83.7	2.56	0.94	13.2	11.7
WetD Sulf.		630	4.0	2.3	70.2	64.2	0.01	0.00	0.16	0.14
WetD Amm.	NADP	630	−7.7	−3.2	70.1	66.3	0.00	0.00	0.03	0.03
WetD Nitr.		630	−44.7	−38.3	57.0	55.4	−0.09	−0.07	0.11	0.11
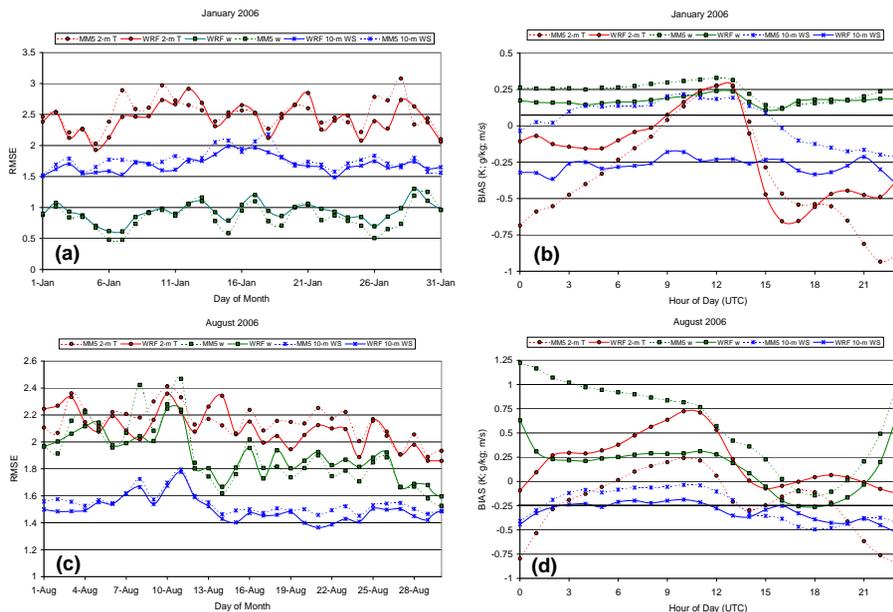
Fig. 1. Daily RMSE (left column) and hourly (UTC) bias (right column) of 2-m T (red; K), w (green; g/kg) and 10-m WS (blue; ms^{-1}) for the MM5 (dashed) and WRF (solid) simulations for January (top) and August (bottom) 2006.
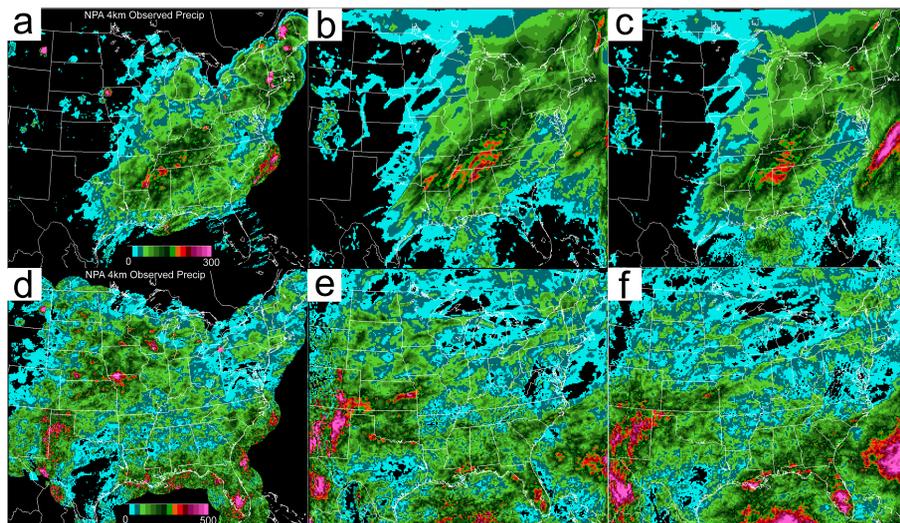
Fig. 2. Monthly accumulated precipitation (cm) for NPA observed (left column), MM5 predicted (middle column) and WRF predicted (right column) for January (top) and August (bottom) 2006.
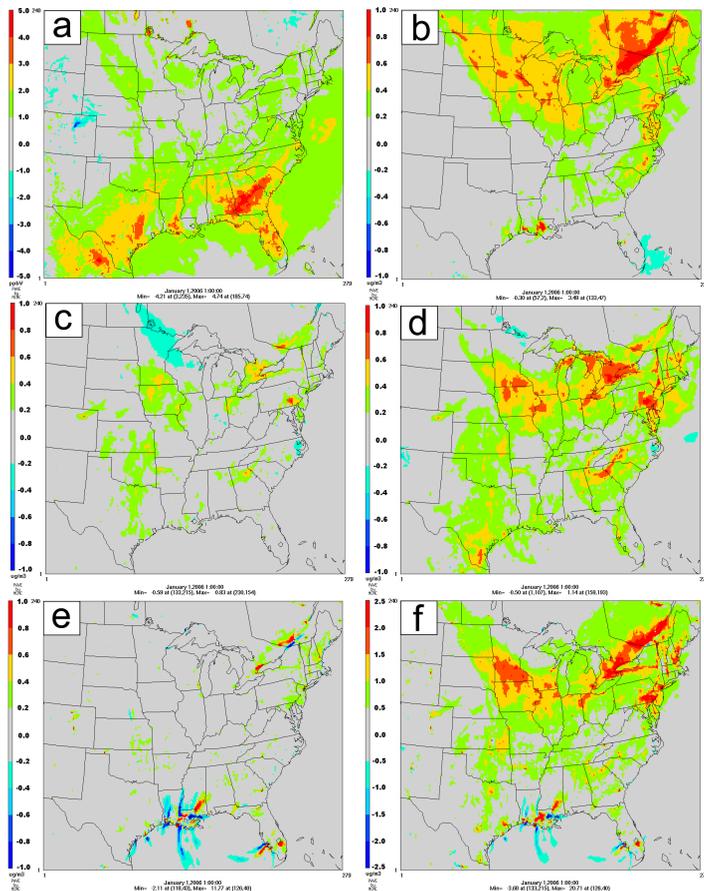
Fig. 3. Monthly average difference in **(a)** O_3 (ppb; upper left) **(b)** SO_4^{2-} ($\mu g/m^3$; upper right) **(c)** NO_3^- ($\mu g/m^3$; middle left) **(d)** TNO_3 ($\mu g/m^3$; middle right) **(e)** TC ($\mu g/m^3$; lower left) and **(f)** total $PM_{2.5}$ mass ($\mu g/m^3$; lower right) for January 2006.

Fig. 4. Monthly accumulated difference in **(a)** precipitation (cm; upper left) **(b)** SO_4^{2-} wet deposition (kg/ha; upper right) **(c)** NO_3^- wet deposition (kg/ha; lower left) and d) NH_4^+ wet deposition (kg/ha; lower right) for January 2006.
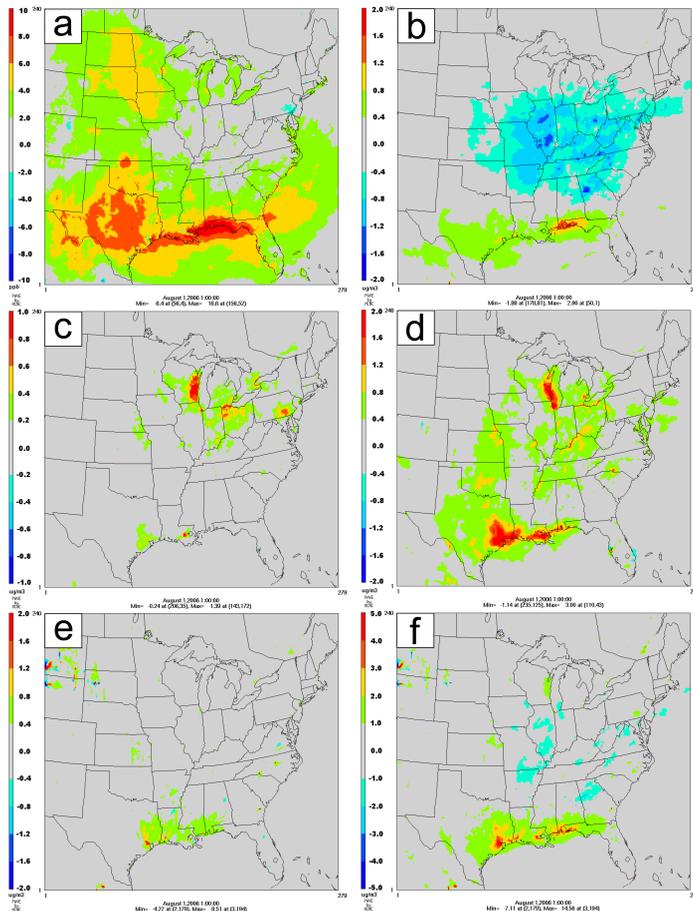
Fig. 5. Monthly average difference in **(a)** O_3 (ppb; upper left) **(b)** SO_4^{2-} ($\mu g/m^3$; upper right) **(c)** NO_3^- ($\mu g/m^3$; middle left) **(d)** TNO_3 ($\mu g/m^3$; middle right) **(e)** TC ($\mu g/m^3$; lower left) and **(f)** total $PM_{2.5}$ mass ($\mu g/m^3$; lower right) for August 2006.

Title Page

Abstract | Introduction

Conclusions | References

Tables | Figures

|◄ | ►|

◄ | ►

Back | Close

Full Screen / Esc

Printer-friendly Version

Interactive Discussion
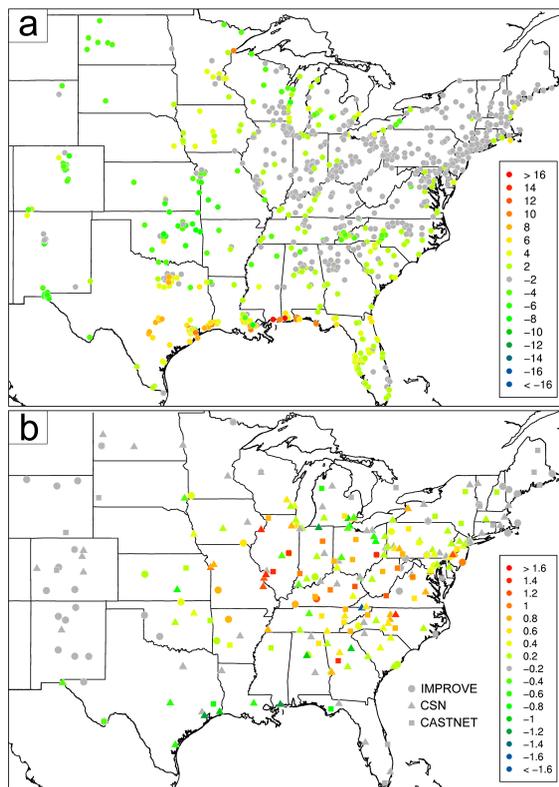
Fig. 6. Average difference in the mean bias between the MM5-CMAQ and WRF-CMAQ simulations for **(a)** maximum 8-h average O_3 (ppb) at the AQS sites and **(b)** SO_4^{2-} (μg/m^3) at IMPROVE (circle), CSN (triangle) and CASTNet (square) for August 2006. Warmer shading represents higher bias in the WRF-CMAQ simulation; cooler shading represents lower bias in the WRF-CMAQ simulation; gray shading represents a difference in mean bias of less than 2 ppb or 0.2 μg/m^3 between the two simulations.
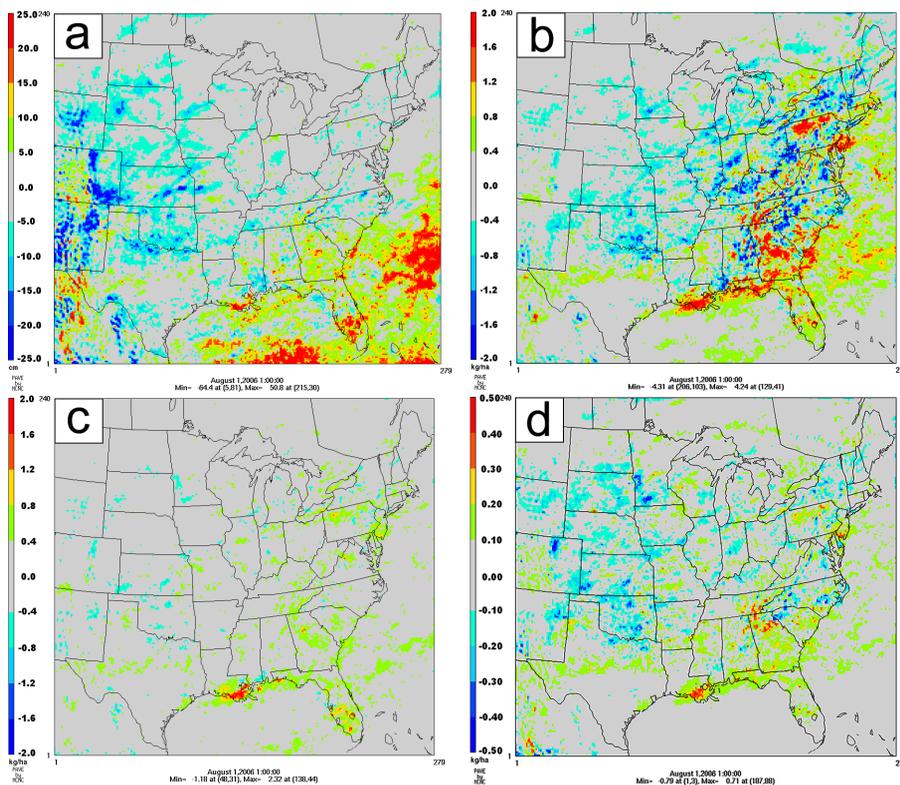
Fig. 7. Monthly accumulated difference in **(a)** precipitation (cm; upper left) **(b)** SO_4^{2-} wet deposition (kg/ha; upper right) **(c)** NO_3^- wet deposition (kg/ha; lower left) and **(d)** NH_4^+ wet deposition (kg/ha; lower right) for August 2006.

Full Screen / Esc